Developing High-Energy Laser-Driven Bremsstrahlung Radiation Sources for Imaging and Analysis of Nuclear Waste Packages – 17300

Christopher P. Jones*, Ceri M. Brenner**, Camilla A. Stitt*, Chris Armstrong**,***, Seyed R. Mirfayzi****, Hamad Ahmed****, Nicholas M. H. Butler***, Adam Higginson***, Charilaos Paraskevoulakos*, Anna Adamska******, John Jowsey******, Paul McKenna***, Satya Kar****, Thomas B. Scott*

*Interface Analysis Centre, HH Wills Physics Laboratory, Tyndall Avenue, Bristol, BS8 1TL, UK

**Central Laser Facility, STFC, Rutherford Appleton Laboratory, Didcot, Oxon, OX11 0QX, UK

***Department of Physics, SUPA, University of Strathclyde, Glasgow G4 0NG, UK

****Centre for Plasma Physics, Queen's University Belfast, Belfast BT7 1NN, UK

*****Department of Physics, University of York, York YO10 5DD, UK

******Ground Floor North B582, Sellafield Ltd, Seascale, Cumbria CA20 1PG

ABSTRACT

Radiographic imaging of small scale simulated nuclear waste packages (a 28mm uranium penny encapsulated in grout) was achieved using a single pulse exposure from an x-ray source driven by a high-power laser. The high-energy laser pulse was generated at the Vulcan laser facility, which focused the photon burst onto a tantalum target foil in order to produce a bright burst of highly penetrating x-rays (with energy >500keV) from a source size less than 0.5mm. The sample was imaged using BAS-TR and BAS-SR image plates alongside a Thalium doped Caesium Iodide scintillator-based detector coupled to CCD chips for rapid image acquisition. The penny was resolved to sub-mm accuracy over a 30cm^2 scan area from a single shot. In addition, on a parallel beamline, neutron generation (of 10^7-10^9 neutrons per steradian per pulse) was achieved, thereby demonstrating the potential application for criticality testing of waste packages.

The principle concern regarding intermediate level waste (ILW) containers is the internal volumetric expansion due to the formation of corrosion products. Therefore, simulated waste samples with hydride corrosion have been formed and characterised in order to emulate this phenomenon. In addition, samples containing controlled isotopic ratios have been formed. This next generation of simulated waste samples have been produced in preparation for a second phase of analysis at the Vulcan laser facility to quantify the identification ability of radiographic imaging and characterisation accuracy of neutronics measurements. This feasibility study successfully demonstrated non-destructive radiography of encapsulated, high density, nuclear material and this paper details the next phase of technological development.

INTRODUCTION

Background

The majority of the UK's nuclear waste is currently stored at Sellafield in Cumbria, where a number of different storage strategies are applied depending on the nature of the waste form. The inherent high radioactivity and unpredictable corrosion products, present after decades in storage, mean that it is exceptionally difficult to accurately analyse basic parameters to describe the waste contents. These parameters include morphology, radioactivity, reactivity and chemical composition of the waste including any associated hazards such as gaseous hydrogen production. Therefore, research and development of investigative technologies is of paramount importance in order to define the risks posed by certain storage scenarios. The analytical difficulties exist because the nuclear waste is contained within vessels opaque to most standard forms of imaging and held in inaccessible areas due to the high radioactivity present.

As of 1st April 2013 the reported volume of radioactive waste in storage in the UK was approximately 216,000 tonnes[1]. Of this, 120,000 is intermediate level waste (ILW), and approximately 28,000 cubic metres have been packaged, producing about 54,000 containers that are held in modern engineered stores. This ILW has been the focus of this feasibility study and subsequent technique development. The ILW containers arising from the processing of spent fuel from Magnox reactors consists of 500L stainless steel drums (weighing approximately 1.2 tonnes when full) in-filled with Magnox cladding, aluminium, uranium and steel, encapsulated in a grout mixture of Ordinary Portland Cement (OPC) and Blast Furnace Slag (BFS). Although these were originally designed to last for 'at least 50 years' [2, 3], recent inspections have shown that following long term storage (>30 years) a portion of these containers are exhibiting deformation, anticipated to be a direct result of the metallic corrosion of the encapsulated ILW. The development of analysis techniques capable of probing the container to discern more information about the underlying causes of external deformation is of paramount importance. Without this data, management of these particular containers is thwarted and, therefore, suitability for future interim storage (≤150 years) is called into question even if the waste is repackaged.

The external deformation of the waste containers, due to the volumetric expansion via metallic corrosion, greatly increases the probability of a localised containment breach. Such a catastrophic even is most likely to occur during transportation, which includes the associated risk of an impact event. Similar storage environments have shown that the potential production of pyrophoric material is a recognised risk within these containers [4, 5]. The legacy wastes at Sellafield site present further examples where limited material knowledge has hindered the processing of wastes and its storage.

There is a requirement to accurately characterise and evaluate the suitability and stability of current techniques for storing and repackaging of nuclear waste for both transport and disposal in a geological facility. At present two approaches are underway in an attempt to characterise the waste; direct investigation of the waste, and analytical studies of simulated waste to determine predictive corrosion rates and the mechanisms occurring within. This project overarches both approaches by

developing an analysis technique for simulated nuclear waste samples over the course of development, whilst the end goal is a fully functioning, diode pumped laser system, capable of direct investigation of the 500L drums currently housed at Sellafield Ltd. The initial feasibility study (reported here) demonstrated the potential for using laser-driven x-ray beams as a future means of examining the internal state of radioactive waste containers. Depending on the target material composition, the photon-matter interaction produces either a bright pulse of highly penetrating x-rays for radiographic imaging, or a pulse of neutrons. The Vulcan laser facility has the capability of producing x-rays with sufficient energy (~500keV+) to penetrate real world storage containers such as the 500L waste drums thus providing a means of identifying the corrosion products formed within. Adjustment to the choice of target material enables the ability to generate neutron bursts with significant flux. These neutrons bursts, when incident on the nuclear waste sample, will interact with the fissile material and provide the means for criticality testing of the waste containers. This analysis is achieved by quantification of the secondary neutron energies produced. This analysis is predicted to provide a quantifiable value of the isotopic composition of fissile material within the sample, thus performing criticality testing of a waste container from a single laser pulse.

The reported study produced radiographic data of simulated Magnox ILW waste material, with several single pulse exposures from the laser-driven source. In addition the Vulcan laser system demonstrated successful neutron generation between 10^7-10^9 neutrons per steradian per pulse which at increased shot rates would generate a suitable source for isotopic quantification of the waste containers. The feasibility study investigated samples comprised of a single Magnox uranium penny encased in concrete with corrosion products too thin to identify with a single shot acquisition. In order to further ascertain the potential for this technique on real world systems, simulated waste samples, with varying levels of oxygen and hydrogen corrosion, have been produced and characterised both prior to and following encapsulation in ordinary portland cement (OPC). In addition a range of samples with pre-determined ratios of U-235 to U-238 have been produced. The next stage of this project will be a similar study of these more complex systems on the Vulcan laser facility, including a 50L drum filled with various metals and concrete. This study will aim to quantify the laser systems capability of discerning between metals and corrosions products, the lateral resolution capability when integrating over multiple scans with background subtraction, and finally the accuracy to which criticality testing of the waste can be performed.

With recent developments of high-power laser systems, to 10Hz operation with the energy levels required for gamma-ray production, a laser-driven multi-modal beamline for waste monitoring application is envisioned.

EXPERIMENTAL METHODS

Sample Production

Phase 1:

For the original feasibility study samples of magnox uranium were cut into pennies with 28mm diameter and thickness of 2mm from an unused, un-irradiated, Magnox

fuel rod (Fig. 1a). The sample was encapsulated in Lafarge ready-mix concrete within a plastic surround (Fig. 1b). The penny was not treated prior to encapsulation and retained an as-received corrosion layer of uranium oxide. Subsequent Focused Ion Beam (FIB) analysis of the oxide layer on samples with the same provenance estimated the thickness to be approximately 2-3µm and ostensibly uniform across the sample surface.

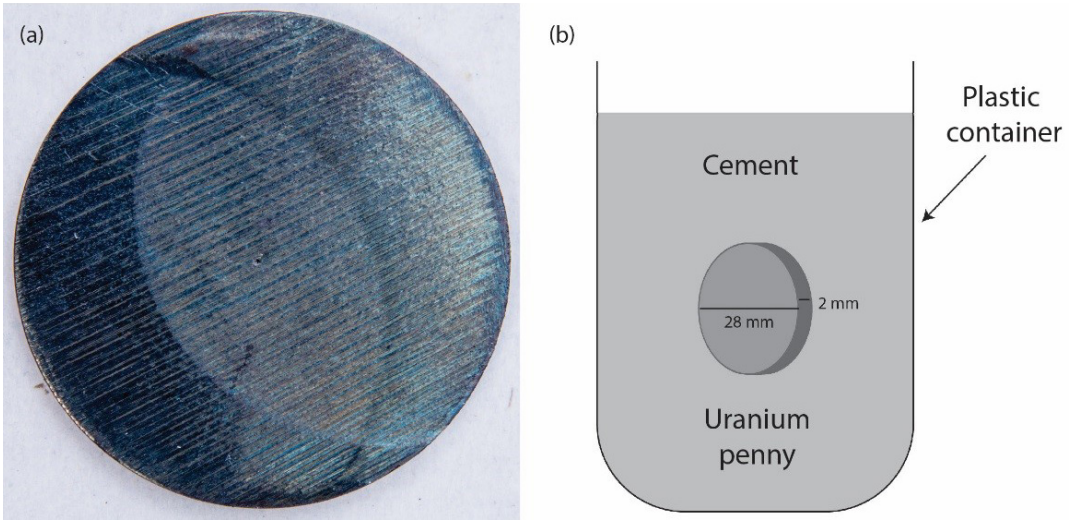

Fig. 1. a) An optical image of the uranium metal penny. b) A schematic diagram of the entire sample.

Phase 2:

For the next stage in development, samples of magnox uranium with various levels of controlled corrosion, by hydrogen (and in the near future with oxygen), as well as samples with various ratios of U-235 to U-238 and large scale samples with non-active components. These have been produced in order to quantify the capabilities of a fully developed system aimed at monitoring intermediate level waste barrels but with the potential for a whole host of analytical applications. Prior to experimentation, samples were mechanically polished using successively finer grades of silicon carbide paper to a P2500 polish. This was performed regardless of the corrosion or encapsulation method in order to remove the surface oxide formed during long term storage.

Two samples were briefly air dried using a blower system and sealed into a stainless steel high-vacuum cell, evacuated to $<1\times10^{-6}$ mbar and heated to 75°C overnight to remove the majority of adventitious water absorbed from the atmosphere or the polishing process. The cell was heated to 240°C and allowed to equilibrate for a two hour period before the admittance of gas to start the hydriding reaction. D_2 gas (at 500mbar pressure) was added to the reaction cell and the adjoining pipework which had a total volume of 157cm^3. The volume was then sealed and the gas pressure monitored in order to observe the onset of hydride formation and control the extent of reaction. Hydriding was halted by evacuating the cells after a calculated hydrogen pressure drop had occurred to result in either 1% or 5% of the total sample converting to UD_3. The samples were subsequently

allowed to cool under high vacuum (<10^{-6}mbar) before analysis and final encapsulation in Ordinary Portland Cement (OPC).

Individual quarter penny samples were encapsulated in OPC (following the standard mechanical polish) and allowed to dry over several days in air prior to loading into a custom stainless steel high vacuum cell. The cell was evacuated to <1×10^{-6}mbar, heated to 240°C and exposed to 500mbar of hydrogen (D_2) and allowed to corrode. In the sample procedure conducted on non-encapsulated samples, hydriding was halted by evacuating the cells after a calculated hydrogen pressure drop had occurred to result in either 1% or 5% of the total sample converting to UD_3. The samples were subsequently allowed to cool under high vacuum (<10^{-6}mbar) prior to extraction and ready for analysis on the Vulcan laser system in 2017.

Characterisation Techniques

EBSD analysis:

Samples were mechanically polished to the standard P2500 grit finish, then further polished to 1µm using diamond polishing paste. These samples were loaded into an electropolishing arrangement and cleaned for 3 minutes with a current density of 1mA/mm^2 in an electrolyte solution consisting of 10:6:6 ratio of research grade ethanol, orthophosphoric acid and ethylene glycol respectively. After washing in methanol to remove acid residues, specimens were rapidly transferred into a scanning electron microscope fitted with an EBSD system.

A Zeiss EVO MA10 equipped with LaB6 electron source and TSL-EDAX instrumentation was used for crystallographic electron backscatter diffraction mapping (EBSD) of the electropolished surface. EBSD data were recorded using OIM™ software for both data capture and analysis. The metal was mapped using structural data provided from the standard TSL database for orthorhombic α-uranium. Where necessary, the raw EBSD data recorded during mapping runs were cleaned using standard OIM™ clean-up functions (nearest neighbour correlation and grain dilation functions).

FIB and SEM analysis:

FIB sectioning of hydrides and subsequent Secondary Electron Microscopy (SEM) imaging were performed on a FEI Helios X600 with Ga+ focused ion beam and high resolution Elstar™ electron column with a Field Emission Gun (FEG) electron source. Samples were cross-sectioned using high focused ion beam currents (up to 20nA) at 30kV. Imaging was attained using the FEG operating at 30kV for identification of the corrosion layer with imaging captured using the Secondary Electron (SE) detector. In addition, the focused ion beam was utilised for imaging the section face. Operation at low currents, and imaging using the SE detector, greater contrast was achieved between the metal and the formed corrosion products.

Optical analysis:

A Sony a6300 with 50mm prime lens and +10 hoya filter was used for large area imaging of the samples attaining ~100µm resolution. Images were captured at medium aperture between 9-14 f-stop and dwells times ranging from 2.5-15 seconds depending on the lighting conditions.

X-Ray Generation

A laser pulse with a peak intensity $\geq 10^{18} W/cm^2$ is focused onto a solid matter target under vacuum, the surface is instantaneously fully ionised to form a high density plasma. The laser electric field then interacts with the charged particles within the plasma state and accelerate a high-current (mega Ampere) of electrons in the laser forward direction. The generated electron beam has a Maxwellian spectral distribution and a bulk temperature up to several MeV, rendering the beam relativistic. This beam in turn generates a bright burst of Bremsstrahlung x-ray radiation as the electrons interact with the atomic structure of the target material. The use of thin, high atomic number target foils (i.e. tantalum and gold) will result in a particularly high peak intensity and energy of Bremsstrahlung radiation, thus generating a large flux of high-energy x-rays required for imaging nuclear waste containers. Dose measurements made during gold target irradiation with the Vulcan laser, at the Science and Technology Facilities Councils Rutherford Appleton Laboratory, show a total beam dose of 43mGy/pulse at 1m[6].

Experimental Setup

X-ray pulses for radiographic imaging were generated during laser-solid interactions with the Vulcan laser at the Rutherford Appleton Laboratory, Harwell Campus. P-polarised, 1054nm wavelength pulses[7] of 10 picoseconds duration delivered 150J of laser energy onto 100µm thick tantalum foil targets at a 20 degrees angle of incidence. In this configuration, the Bremsstrahlung energy spectrum peaked at 200keV, above which the photon flux logarithmically decreased. Spectrometer readings measured an x-ray beam with a bulk temperature of 600keV[8] during radiographic imaging. Systematic variations in the incident laser energy are shown to directly correlate with the energy of the produced gamma rays[8]. This simulation demonstrated that gamma rays of >2MeV were expected to be generated in this current configuration. Contrast radiographs were obtained using BAS-TR and BAS-SR image plate (IP) detector films to capture the x-rays after transmission through the sample. For rapid image acquisition, a recently developed 2D active scintillator based detector, constructed of Thalium doped Caesium Iodide (CsI) pixels of dimensions 500×500µm and a thickness of 1cm, optically coupled to CCD chips, with full working area of $30cm^2$, was also operated. Whilst the image quality is noisier with less contrast it provided rapid, near instantaneous, image acquisition when compared to the traditional IP film, for which digitising the signal at high resolution can take up to an hour for a single 20cm×40cm piece.

A 1.6cm thick copper filter was positioned in front of the scintillator array, attenuating x-rays of energy below 110keV, in order to energy-select the irradiation onto the scintillator array (Fig. 2). The IP was left unfiltered so as to absorb all x-rays penetrating through the test objects, although, the IP has a peak sensitivity to x-rays with energy 50keV and is weakly attenuating for those >100keV. An aluminium filter was trialled to filter out energies below 40keV but this was not seen to improve the quality of the collected data. The sample was located externally to the vacuum interaction chamber, level with the laser axis, at a range of distances in front of the detector plate in order to enable imaging at various magnification factors (Fig. 2). Contact radiography (magnification 1) of the test object was conducted with the IP detector placed directly behind the object plane

whilst high magnification (greater than a factor of 5) was carried out by extending the distance between the object and the CsI detector plane to 2.2 metres.

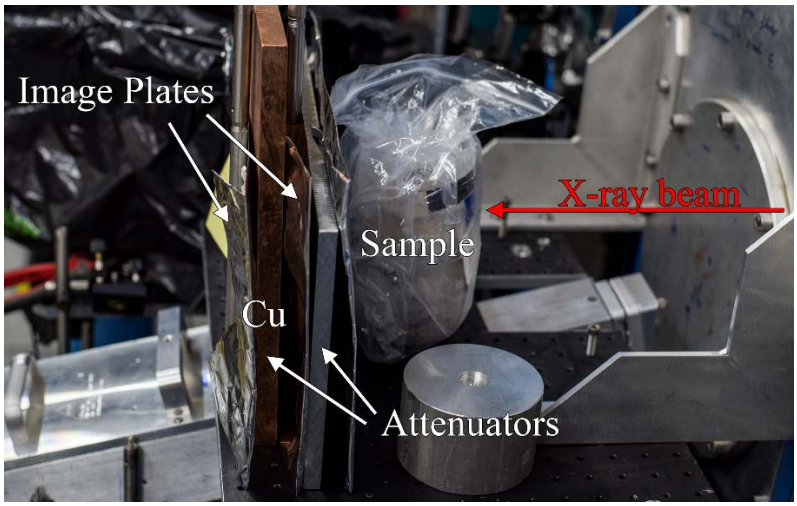

Fig. 2. A photograph of the experimental arrangement; the position of the sample, image plates and filters with respect to the x-ray beam are displayed, whilst the CsI detector is positioned ~2m away from the sample.

RESULTS

Results of Phase 1:

Crystallographic microstructural characterisation of Magnox uranium:

Fig. 3 presents EBSD analysis of the magnox uranium metal exhibiting crystalline grains with diameters of the order of 100µm divided by subgrains of approximately 20-40µm diameter. As expected, carbonitride inclusions are also present, distributed relatively homogenously across the surface of the metal.

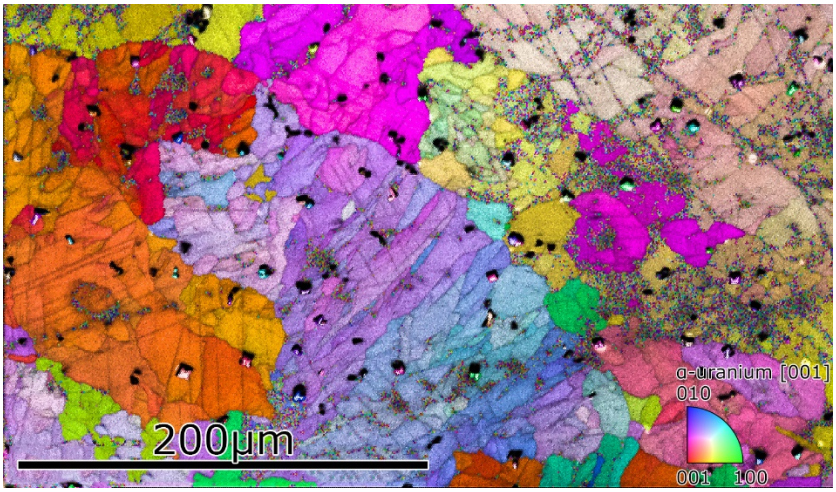

Fig 3. Combined SE and Inverse Pole Figure (IPF) map showing the distribution of grain size, sub-grain boundaries and carbide inclusions (small dark squares 5-10µm in width).

As-received oxide layer:

The as-received magnox uranium was sectioned using the FIB to reveal the extent of oxidation corrosion during storage. Samples exhibited a relatively uniform oxide layer 2-3µm thick (Fig. 4). Distinguishing the oxide layer from the metal was achieved by FIB raster scanning of the section face using a 90pA probe current revealing the crystallographic variations in the metal. This is in contrast to the fine structured oxide layer which appears ostensibly uniform in secondary electron intensity.

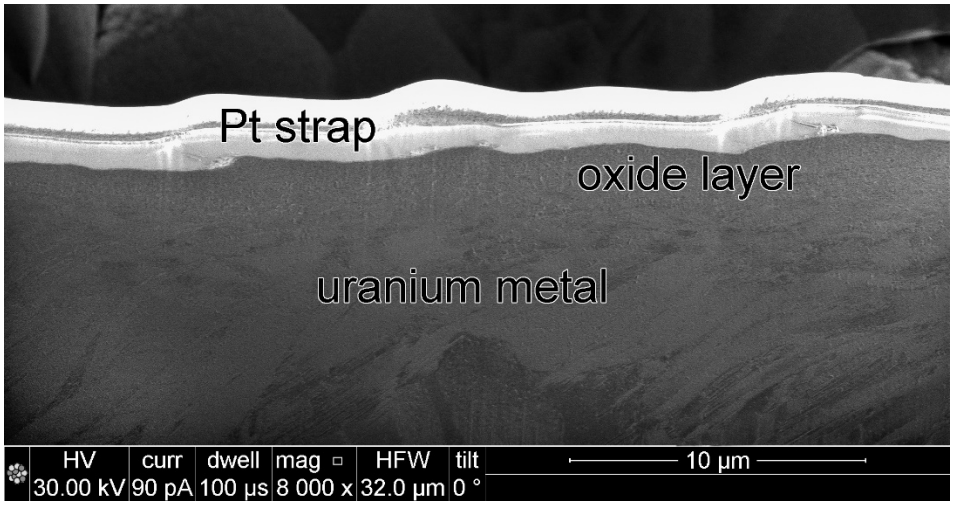

Fig. 4. SE image of a FIB section through the 2-3µm thick oxide layer into the uranium metal. The distinction between oxide and metal is evident by the crystalline twins present in the metal.

Radiographs of the cement encapsulated uranium, using the IP and CsI detectors, and are displayed in Figs. 5, 6 and 7 with basic image processing applied to increase brightness and contrast. Using both detectors, the outline of the uranium penny was clearly resolved regardless of the cross sectional thickness and at both low and high magnification factors. The high magnification CsI detector radiographs achieved a lower contrast ratio due to several factors, the photon intensity is reduced due to the distance from the source (>2m), the CsI detector is not as sensitive as image plates, and the 1.6 Cu attenuator absorbed a high proportion of the beam energy.

As expected the surrounding grout was observed to be intact with no apparent fracturing since the corrosion products were predominantly formed prior to encapsulation. In both examples, the spatial resolution and absorption contrast of the radiographs was insufficient to identify the 2-3µm thick, as-received, uranium oxide layer. This was also expected since projection radiography, at a magnification factor of 5, onto the CsI array of a 5mm thick tungsten resolution test grid demonstrated that features of size 200µm were resolved [8], however, these were larger features exhibiting a greater contrast ratio. This initial investigation successfully demonstrated the first radiographic imaging of encapsulated uranium metal pennies using a single pulse exposure from a laser-driven x-ray beam.

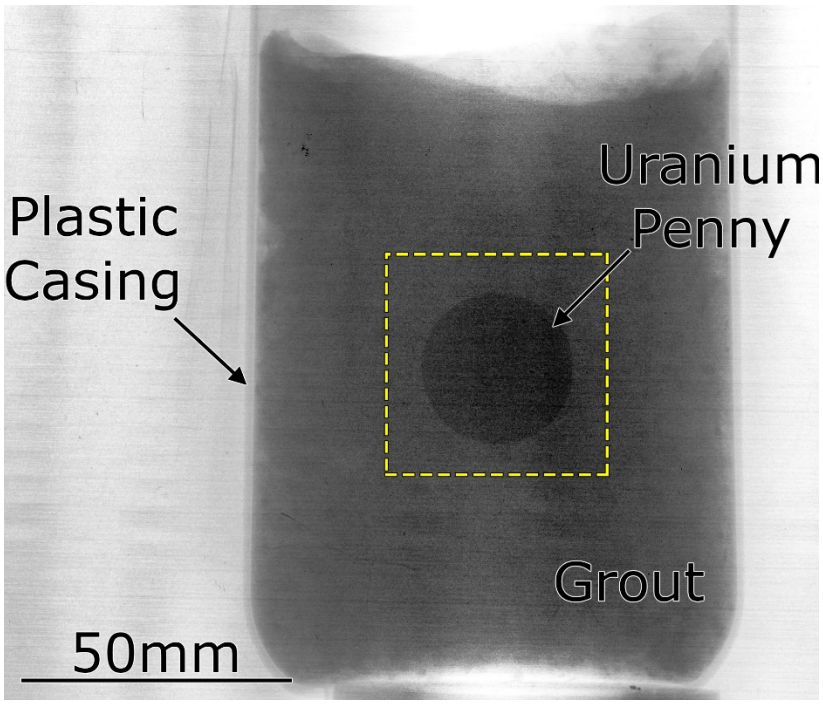

Fig 5. Raw signal from a single pulse exposure radiograph of the entire sample in front of an, unfiltered, image plate detector (IP). The outline of the plastic container, cement and uranium penny are clearly identified. The high dynamic range of the image plate detector reveals absorption contrast even between materials of dramatically different attenuation factor.

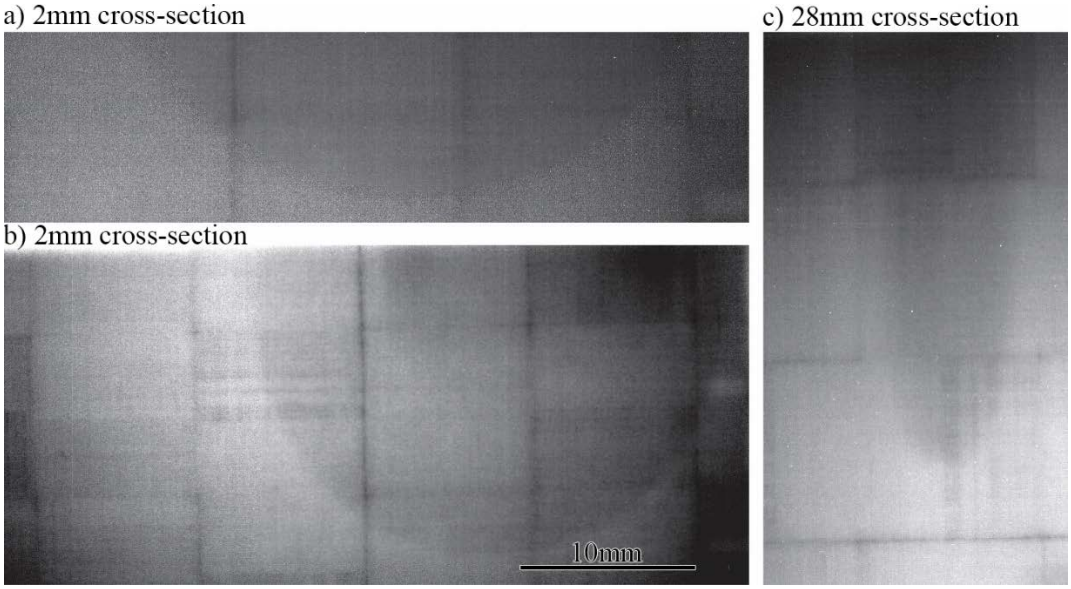

Fig 6. Projection radiography recorded using the CsI detector with an additional Cu attenuator (magnification factor of ~5) displaying the uranium penny through the thinnest (a-b) and thickest (c) cross sections. The grid-like structure seen in the radiograph is an artefact from the tiled structure of the CsI array.

Fig. 7 displays contact radiography at a range of orientations. By reducing the rotation angle between acquisitions and, therefore, increasing the number of images, a 3D tomographic picture of the waste can be calculated. Similar measurements have been conducted at Diamond Light Source (DLS) to capture x-ray tomographic data and x-ray diffraction data from smaller samples requiring less penetrating x-ray energies (e.g. Fig. 8).

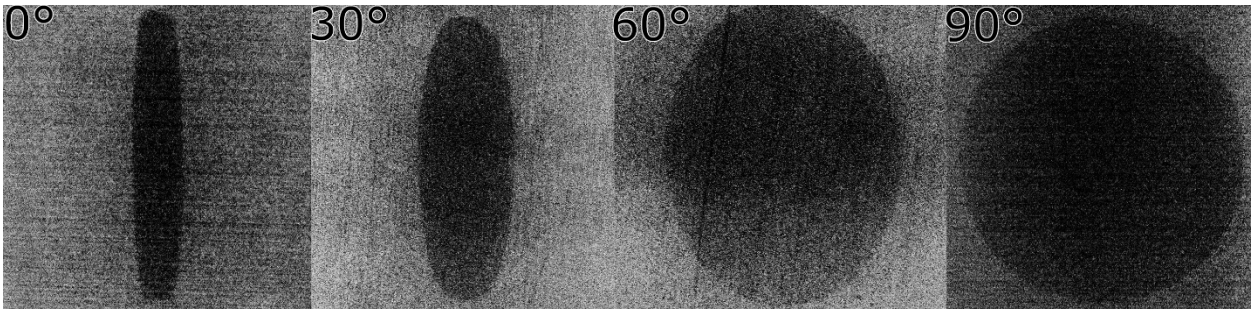

Fig 7. Contact radiography at various angles to illustrate the type of data required for tomographic analysis (0-180° is required for a complete 3D reconstruction of the sample).

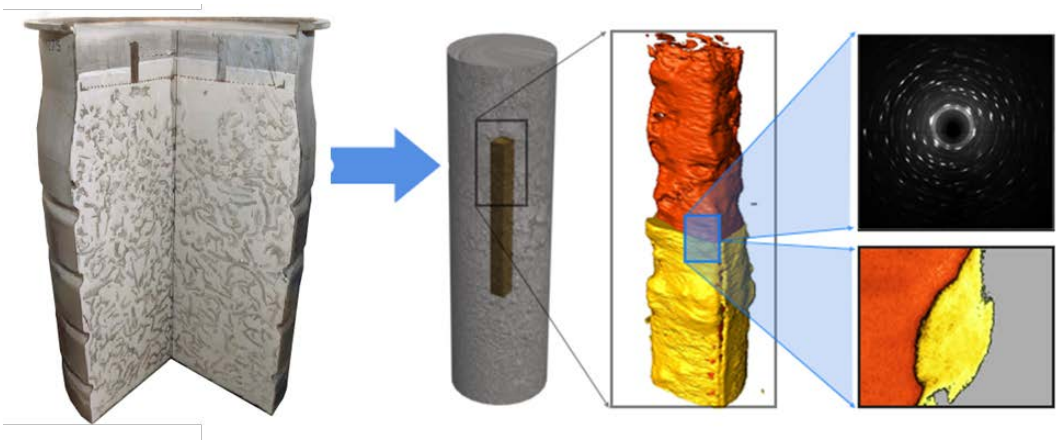

Fig 8. The concept of using synchrotron x-ray tomography and selected volume diffraction to provide direct investigation of uranium metal as it corrodes inside a small simulant waste package. Tomographic data and diffraction patterns are from the work of stitt et al [9]

By directing the laser onto a parallel beamline, a highly penetrating neutron beam (with an incident energy of 1-5MeV) was generated [8]. A flux of 10^7-10^9 neutrons per steradian, per pulse, was achieved. Fig. 9 displays the time-of-flight signal obtained by oscilloscopes linked to plastic scintillators located within the neutron path[10]. The peak at time t=0 saturated the detector and is a result of relativistic signal which arises from the initial x-ray flash from Bremsstrahlung emission. This peak provides evidence for x-ray generation in the desired energy regime (>500keV), in situ and in line with neutron beam generation, since the scintillators were positioned two meters from the source and shielded by 10cm thick lead bricks which could only be penetrated by such high-energy photons. The increase in signal intensity between 100-200ns indicated that radiation propagated at non-relativistic

speeds but achieved penetration of the lead shielding, thus indicating the successful generation of neutron irradiation.

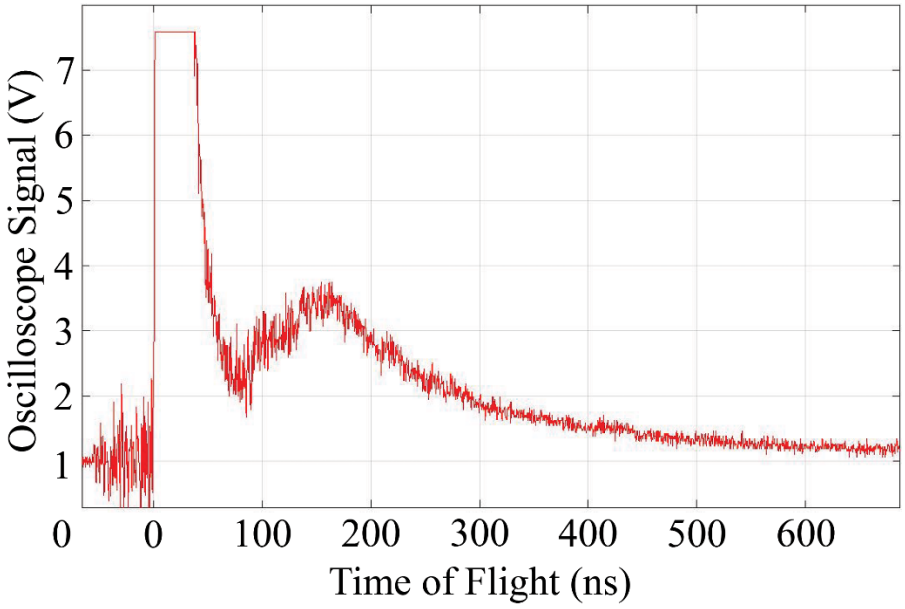

Fig. 9. The raw data recorded by oscilloscopes of the neutron time-of-flight signal.

Characterisation of Samples for Phase 2:

Hydrided samples:

Optical imaging of samples (Fig. 10) revealed a thin hydride layer with some larger spot hydrides for the 1% sample (a). 5% hydriding resulted in significant spalling of the surface, the remaining coupon exhibits a fairly uniformly corroded surface with conglomerate particles several hundred microns in diameter (b).

FIB sectioning and SE imaging of the formed hydrides revealed a hydride layer approximately 10µm thick with blisters up to 30m thick in the 1% hydride sample (Fig. 11a). Sectioning of the 5% hydrided sample revealed large fragmented growths approximately 100-300µm in thickness at regular intervals across the surface (Fig. 11b). The entire sample was coated in a 20µm thick adhered hydride layer only twice as thick as the 1% reacted sample.

Following the hydrogen corrosion of uranium, the samples were encapsulated in LaFarge™ ordinary portland cement (OPC). Similar samples containing polished, non-corroded, uranium metal, have also been encased in OPC in preparation for encapsulated corrosion experiments.

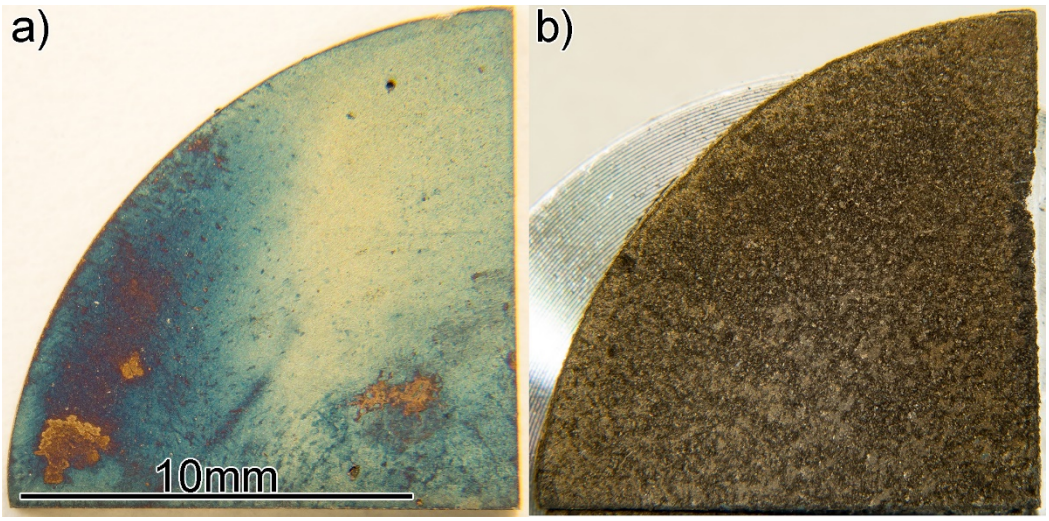

Fig. 10. Optical images of hydrided, quarter magnox uranium coupons. a) 1% sample conversion. b) 5% sample conversion prior to encapsulation.

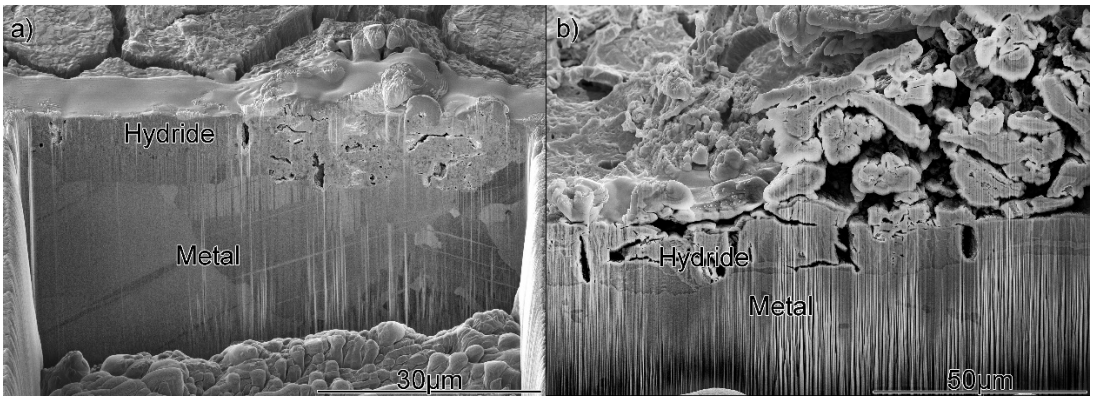

Fig. 11. SE images of a) 1% hydrided Magnox uranium b) 5% hydrided Magnox uranium.

DISCUSSION

This feasibility study successfully demonstrated non-destructive radiography of encapsulated high density nuclear material using the Vulcan laser system to drive high-energy x-ray beam generation. The laser pulse driven x-ray source was found capable of penetrating small, yet significant, masses of material, successfully achieving imaging spatial resolution to approximately 200µm[8] over wide scan areas of ~30cm^2. This laser-based method of generating high-energy x-ray and particle beams, therefore, exhibits great potential for further development of additional techniques including x-ray tomography, gamma-ray tomography, neutron imaging and criticality testing.

The samples for this initial phase of testing were limited to a native oxide thickness of only 3µm. The samples produced for phase 2 of this project, however, were found to exhibit extensive corrosion products with an average thickness of 20µm but with regular surface features up to several hundred microns in size. Samples containing controlled ratios of U-235 to U-238 by controlling the mass of natural to depleted uranium encased in grout will provide suitable known targets for

characteristic neutronics work. These encapsulated samples will provide suitable reference material for the next stage of the project to be conducted at the Vulcan laser facility in 2017.

Advantages of a Laser Driven Source

Laser-driven, pulsed, x-ray sources are well suited for non-destructive testing applications in security and high value sectors, such as nuclear, aerospace and advanced manufacturing[8]. High lateral resolution imaging of large, dense, objects is attainable due to the high-energy (>500keV), high-flux (43mGy) delivered in each laser pulse in conjunction with the small size (<0.5mm) of the source emission area. Laser driven sources provide these unique characteristics when compared to their commercially available counter parts, such as linac systems, which deliver these qualities in a single source. The laser-driven system is, therefore, well suited to provide the advanced inspection techniques required in nuclear waste management, offering the potential for a ground-breaking analytical technique, of particular interest to the nuclear sector.

In the present experiment the x-ray beam demonstrated large divergence which permits a large field of view, thus providing a suitable foundation for the development of tomographic imaging of large objects. Simultaneous production of high-energy, bright neutron beams provides the potential for neutron radiography; a non-destructive, element specific, imaging technique, which is particularly sensitive to large variations in atomic number [11].

Potential for Nuclear Waste Scanning Facility

Adequate nuclear waste scanning requires the identification of the approximate mass and spatial distribution of i) high density material, ii) sensitive corrosion products, iii) fissile material, iv) pyrophoric material and v) any significant gas pockets or voids. This experiment has shown that laser-driven photon sources have the capability to identify the distribution of material based on relative mass, from the stark difference between uranium and cements attenuation of the x-rays.

Real ILW containers often exhibit external deformation which is likely caused by expanding material located near the circumference. This is ascribed to volumetric expansion driven by corrosion of contained metal waste located close to the drum walls. These materials pose the greatest risk to the safe confinement of nuclear waste since they are both radioactive and hydrogen based, (e.g. hydrogen gas or metal hydrides). Neutrons are highly sensitive to hydrogen based compounds, thus neutron imaging will be able to efficiently identify their location and relative quantity [12]. Neutrons have also previously been utilized for criticality testing, for example by the nuclear materials identification system (NMIS)[13]. In this method, a time resolved analysis is achieved; neutrons that pass through active material induces fission, generating additional particles that are detected later than directly transmitted neutrons.

The limiting factor for the current system is shot frequency (approximately once every 20 minutes using the Vulcan laser system). In order to reduce image noise several shots need to be taken of the system to provide background subtraction and image integration functions. In addition, tomographic analysis requires a large number of images per sample to be acquired through a 180° rotation. Therefore,

the use of a high-power diode-pumped laser, such as the DiPOLE system [14], is required. This not only offers the same high-power that the Vulcan system provides, but can generate pulses at 10Hz operation and is more efficient, more compact, and is, therefore, more deployable in a nuclear facility.

CONCLUSIONS

This experiment has provided proof of concept for the development of laser induced gamma ray burst tomography and in-situ detection of high density materials in life-sized nuclear waste packages. For the second phase of testing samples have been produced that successfully replicate the formed corrosion products and corresponding density changes on a range of scales. This will successfully test the limits of imaging and identification properties of a laser driven x-ray system in addition to the characterisation ability of neutronics measurements from known ratios of U-235 to U-238.

The implementation of diode pumped lasers provides the capability of multi-modal bursts of high-energy x-rays and neutrons at rates of up to 10 images per second. This will enable both gamma-ray and neutron tomographic analysis of full-scale nuclear waste containers. In addition, scaled up to 10Hz operation, the dose delivery of a laser-driven x-ray beam is 26Gy/min at 1m, which is competitive with even the highest energy market-leading linac systems.

The development and construction of this instrumentation is feasible on a 10 year timescale and holds potential for an in-situ waste scanning capability at nuclear waste storage facilities. Once operational, waste packages displaying errant behaviour will be prioritised for scanning and analysis, whilst standard packages will undergo routine product control and assessment before transportation to a geological disposal site.

FUTURE WORK

The work presented here was a feasibility study to determine the merits of more involved research and development as a step towards a commercial machine capable of 10Hz operation. For real-world waste samples tomographic reconstruction will be required to identify corrosion products amongst the complex and random arrangement inside the canisters. This is attainable in a practical time-frame if multiple images per minute are acquired whilst the waste container is rotated. In addition, the x-ray energy needs to be high enough to penetrate the larger, dense, waste containers.

Therefore, for phase 2 of the project further work is planned on the Vulcan system in 2017. The work is planned into three distinct sections aiming to bring the feasibly study a step closer to a final product to be deployed at Sellafield.

Neutronics Samples:

Grouting of pure natural uranium provides a higher percentage (0.711% U-235, 99.284% U-238, and 0.0055% of U-234 by weight) of fissile material than depleted. By grouting ratios of 100% natural, 50%/50% natural to depleted, and 100% depleted, the fissile content of the samples is controlled and the characterisation ability of neutronics measurements can be calibrated and tested.

The aim is to produce data enabling the accurate quantification of the isotopic ratio of preconfigured samples.

Corrosion Samples:

TABLE I. List of corroded uranium samples:

Batch	Sample	Corrosion	Percentage	Grouted
1	Quarter Magnox	Hydride	1%	After
2	Quarter Magnox	Oxide	1%	After
3	Quarter Magnox	Hydride	5%	After
4	Quarter Magnox	Oxide	5%	After
5	Quarter Magnox	Hydride	1%	Before
6	Quarter Magnox	Oxide	1%	Before
7	Quarter Magnox	Hydride	5%	Before
8	Quarter Magnox	Oxide	5%	Before
9	Quarter Magnox	Hydride	50%	Before
10	Quarter Magnox	Oxide	50%	Before

Table I presents the planned range of corroded sample batches to be produced for analysis at the Vulcan laser facility. The characterisation of corrosion samples up to 5% conversion provide a range of surface features and density changes to challenge the imaging capabilities of the Vulcan laser system. Corrosion of samples at 50% will be conducted on encapsulated samples to test the detection capability of crack formation in the cement matrix, however, pre-corroded samples to this level are irrelevant since the surface corrosion will simply spall at levels greater than 5% conversion.

Large Scale Samples:

Larger, more complex, samples will be produced by infilling a 50L container with grout and a range of dense metals alongside known products expected within the intermediate level waste containers (such as magnesium and aluminium).

ACKNOWLEDGEMENTS

This research was supported by funding from Sellafield Ltd (CoE in uranium and reactive metals), with additional support from the Central Laser Facility and the STFC Business and Innovation Directorate for their funding of the access to the Vulcan laser facilities.

In addition, EPSRC grant number EP/J003832/1 and STFC grant number ST/K502340/1 were used in supporting work from Strathclyde University, while EPSRC grant EP/J002550/1 supported work from Queens University, and finally we would also like to thank the Royal Academy of Engineering for current and onwards support in developing this technology

REFERENCES

Author(s), Title, Year published, and Publication information.

[1] Nuclear Decommissioning Authority, Department of Energy and Climate Change, *Radioactive Wastes in the UK: A Summary of the 2013 Inventory*. ISBN: 978-1-905985-33-3

[2] G. A. Fairhall, J. D. Palmer, *Special double issue proceedings of symposium d of the e-mrs fall meeting 1991 the encapsulation of magnox swarf in cement in the united kingdom*, Cement and Concrete Research 22 (2) (1992) 293-298. doi:http://dx.doi.org/10.1016/0008-8846(92)90068-7.

[3] J. D. Palmer, G. A. Fairhall, *Special double issue proceedings of symposium d of the e-mrs fall meeting 1991 properties of cement systems containing intermediate level wastes*, Cement and Concrete Research 22 (2) (1992) 325-330. doi:http://dx.doi.org/10.1016/0008-8846(92)90072-4.

[4] T. C. Totemeier, *Characterization of uranium corrosion products involved in a uranium hydride pyrophoric event*, Journal of Nuclear Materials 278 (23) (2000) 301-311. doi:http://dx.doi.org/10.1016/S0022-3115(99)00245-7.

[5] T. C. Totemeier, Report 0022-3115, Argonne National Laboratory (June 1995 1995).

[6] R. J. Clarke, D. Neely, R. D. Edwards, et al, *Radiological characterisation of photon radiation from ultra-high-intensity laser plasma and nuclear interactions*, Journal of Radiological Protection 26 (3) (2006) 277.

[7] C. Hernandez-Gomez, P. Brummitt, D. Canny, et al, *Vulcan petawatt-operation and development*, J. Phys. IV France 133 (2006) 555-559.

[8] C. M. Brenner, S. R. Mirfayzi, D. R. Rusby, et al, *Laser-driven x-ray and neutron source development for industrial applications of plasma accelerators*, Plasma Physics and Controlled Fusion 58 (1) (2016) 1.

[9] C. A. STITT, M. HART, N. J. HARKER, K. R. HALLAM, J. MACFARLANE, A. BANOS, C. PARASKEVOULAKOS, E. BUTCHER, C. PADOVANI, T. B. SCOTT, *Nuclear waste viewed in a new light; a synchrotron study of uranium encapsulated in grout*, Journal of Hazardous Materials 285 (2015) 21 221–227.].

[10] S. R. Mirfayzi, S. Kar, H. Ahmed, et al, *Calibration of time of flight detectors using laser-driven neutron source*, Review of Scientific Instruments 86 (7) (2015) 073308. doi:doi:http://dx.doi.org/10.1063/1.4923088.

[11] M. Roth, D. Jung, K. Falk, et al, *Bright laser-driven neutron source based on the relativistic transparency of solids*, Physical Review Letters 110 (4) (2013) 044802, pRL.

[12] P. A. Hausladen, P. R. Bingham, J. S. Neal, et al, Portable fast-neutron radiography with the nuclear materials identification system for fissile material transfers, Nuclear Instruments and Methods in Physics Research Section B: Beam Interactions with Materials and Atoms 261 (12) (2007) 387-390. doi:http://dx.doi.org/10.1016/j.nimb.2007.04.206.

[13] J. T. Mihalczo, J. A. Mullens, J. K. Mattingly, et al, *Physical description of nuclear materials identification system (nmis) signatures*, Nuclear Instruments and Methods in Physics Research Section A: Accelerators, Spectrometers, Detectors and Associated Equipment 450 (23) (2000) 531-555. doi:http://dx.doi.org/10.1016/S0168-9002(00)00304-1.

[14] P. D. Mason, M. Fitton, A. Lintern, et al, *Scalable design for a high energy cryogenic gas cooled diode pumped laser amplifier*, Applied Optics 54 (13) (2015) 4227-4238. doi:10.1364/AO.54.004227.